

Influence of Oxidation in Starting Material Sn on Electric Transport Properties of SnSe Single Crystals

著者	Yamashita Aichi, Ogiso Osamu, Matsumoto Ryo, Tanaka Masashi, Hara Hiroshi, Tanaka Hiromi, Takeya Hiroyuki, Lee Chul-Ho, Takano Yoshihiko
journal or publication title	Journal of the Physical Society of Japan
volume	87
number	6
page range	065001-1-065001-2
year	2018-05-10
URL	http://hdl.handle.net/10228/00007128

doi: <https://doi.org/10.7566/JPSJ.87.065001>

1 **Influence of Oxidation in Starting Material Sn on Electric**
2 **Transport Properties of SnSe Single Crystals**

3 Aichi Yamashita^{1,2†}, Osamu Ogiso^{1,2}, Ryo Matsumoto^{1,2}, Masashi Tanaka^{1,3},

4 Hiroshi Hara^{1,2}, Hiromi Tanaka⁴, Hiroyuki Takeya¹, Chul-Ho Lee⁵, and

5 Yoshihiko Takano^{1,2}

6 ¹WPI-MANA, National Institute for Materials Science, 1-2-1 Sengen, Tsukuba, Ibaraki,

7 305-0047, Japan

8 ²Graduate School of Pure and Applied Sciences, University of Tsukuba, 1-1-4

9 Tennodai, Tsukuba, Ibaraki, 305-8577, Japan

10 ³Graduate School of Engineering, Kyushu Institute of Technology, 1-1 Sensui-cho,

11 Tobata, Kitakyushu, Fukuoka, 804-8550, Japan

12 ⁴National Institute of Technology, Yonago College, 4448 Hikona, Yonago, Tottori 683-

13 8502, Japan

14 ⁵National Institute of Advanced Industrial Science and Technology (AIST), Tsukuba,

15 Ibaraki, 305-8568, Japan

16
17 We found that the electronic transport property of SnSe single crystals was sensitively
18 affected by oxidation in raw Sn. Semiconducting SnSe single crystals were obtained by

19 using Sn of grain form as a starting material while powder Sn resulted in metallic SnSe.
20 X-ray photoelectron spectroscopy analysis revealed that the surfaces of raw Sn were
21 oxidized, which volume fraction is lower in grain Sn. This indicates that the amount of
22 oxygen in raw Sn is the key factor for the electronic transport property of SnSe.

23 SnSe is well-known as a p-type semiconductor for a long time [1-3]. Recently, Zhao et
24 al. reported that SnSe single crystal shows ultrahigh dimensionless figure-of-merit (ZT)
25 values of 2.6 and 2.3 at 923 K in the b and c directions [4]. These high ZT values are
26 achieved with high power factor and extremely low thermal conductivity. After the report
27 in 2014, intense investigations have been conducted by many groups [5-22]. More
28 recently, the ZT values around 2.0 have been reported with Bi-doped n-type and Na-doped
29 p-type SnSe single crystals [5, 16, 17]. However, the reproducibility of the exceptionally
30 high thermoelectric performance has not been obtained to date. Different thermoelectric
31 properties, especially in electrical conductivity, have been reported from several groups
32 for both of single crystalline and poly crystalline samples. Some groups reported metallic
33 behavior in electrical conductivity [16-18]. On the other hand, others reported
34 semiconducting behavior [19-23] and consistent results have not been obtained so far.

35 Motivated to figure out the reason of these different results, we focused on the possible
36 influence of oxygen content in the starting materials of Sn. Herein, we report on the
37 electrical conductivity measurements along the bc plane for SnSe single crystals in a
38 temperature range from 2 to 390 K. It was found that the electrical conductivity was
39 controlled by changing the oxygen content during the synthesis. The electrical conducting
40 behavior changed from semiconducting to metallic with increase of the oxygen content

41 in the raw Sn.

42 Single crystals of SnSe were grown from the congruent melt. Starting materials were
43 Se chips and two different forms of Sn. Grain form Sn (diameter: ~ 3.0 mm) and powder
44 form Sn (diameter: ~ 0.15 mm) with the same purity of 99.99 % were used. To examine
45 the form dependence on electric transport property of grown single crystals, the ratio of
46 grain and powder form Sn was systematically varied (grain Sn : powder Sn = 100 : 0, 90 :
47 10, 70 : 30, 0 : 100). These Sn grains and/or Sn powders and Se chips were loaded into
48 quartz tubes in stoichiometric composition. The tubes were then evacuated and sealed.
49 They were slowly heated to 600°C and kept for 12 hours followed by furnace cooling. As
50 a result, poly crystalline ingot of SnSe was obtained. The obtained ingot was ground and
51 heated to 1000°C and kept for 10 hours in the double sealed evacuated quartz tubes. These
52 double quartz tubes are necessary to avoid the enters of the oxygen by the breaks of inner
53 quartz tube due to stress from the structural transition during furnace cooling. They were
54 cooled down to 840°C in 8 hours followed by furnace cooling. Finally, SnSe single
55 crystals with typical size of $10 \times 5 \times 3$ mm³ were obtained.

56 Powder X-ray diffraction (XRD) patterns were measured by using Mini Flex 600
57 (Rigaku) with Cu-K α radiation. For the measurements, single crystals were ground into
58 powder. Chemical states of raw Sn were examined by X-ray photoelectron spectroscopy

59 (XPS) analysis using an AXIS-ULTRA DLD (Shimadzu/Kratos) with an Al-K α X-ray
60 radiation ($h\nu = 1486.6$ eV), operating at a pressure of 9×10^{-9} Torr. The analyzed area
61 was approximately 1×1 mm². Electrical conductivity was measured using a Physical
62 Properties Measurements System (PPMS, Quantum Design) in the temperature range of
63 2–390 K.

64 XPS analysis was carried out to examine the chemical states of raw Sn in the both grain
65 (red line) and powder (blue line) forms (Fig.1). There is a well-defined peak at 487.5 eV
66 in the XPS spectrum of the Sn 3d, which is associated with the Sn 3d_{5/2} state. This is a
67 characteristic feature of a tetravalent Sn ion (Sn⁴⁺) [24], implying the presence of SnO₂
68 in both grain and powder Sn. Most likely, it could be on the surfaces. The smaller peak at
69 around 485 eV arises from the Sn⁰ state [24], indicating the presence of the non-oxidized
70 metal Sn. The thickness of SnO₂ layer should be less than few nm that is the value of the
71 penetration depth of XPS measurement. These results indicate that by using the powder
72 Sn the larger amount of oxygen content would be included during the synthesis due to
73 larger volume fraction of SnO₂ coming from the larger surface area.

74 Figure 2 shows the X-ray diffraction patterns of pulverized SnSe single crystals grown
75 from grain and powder Sn. Inset shows the enlargement of the (400) reflection. The
76 diffraction patterns of both samples can be indexed with an orthorhombic system of the

77 space group $Pnma$. The lattice constants of a , b and c axes were determined to be $a =$
78 $11.48(7)$ Å, $b = 4.44(2)$ Å and $c = 4.15(1)$ Å for both samples comparable to the literature.
79 Note that there are no peaks related to SnO_2 , indicating that the oxygen content is quite
80 low.

81 Figure 3 shows the temperature dependence of the electrical conductivity of SnSe single
82 crystals along the bc plane. The electrical conductivity strongly depends on the ratio of
83 grain and powder form Sn used as starting materials. The sample from grain Sn 100%,
84 which may contain the smallest amount of oxygen content, showed semiconducting
85 behavior. The conductivity sharply decreased with decreasing temperature. The small
86 electrical conductivity indicates a low hole concentration ensuring the purity of the
87 sample that has small deviation from the ideal stoichiometry. On the other hand, the
88 electrical conductivities increased and their behaviors became metal like with decreasing
89 the ratio of grain Sn and increasing the amount of oxygen content. The electrical
90 conductivity of SnSe grown by 100% powder Sn showed good agreement with that of the
91 reported ones by Zhao et al. [4]. The present results indicate that transport properties of
92 SnSe single crystal can be controlled from semiconductor to metal by varying the ratio of
93 grain and powder form of Sn used as a starting material. This can be due to the difference
94 of the oxygen volume fraction presenting on the surface of both raw Sn. In fact, pure SnSe

95 is known as a p-type semiconductor [1-3], which is in good agreement with our
96 semiconducting SnSe single crystals with the lowest amount of oxygen content. Hole
97 carrier can be doped by the lack of Sn [1]. Our metallic SnSe could also be explained by
98 the increase of hole carrier with increasing the Sn deficiency, which can be caused by the
99 deviation from the stoichiometry due to the oxidization of the surface of raw Sn. In any
100 case the existence of oxygen plays the important role to change the electronic state of
101 SnSe, possibly by interacting with a lone pair or existing in an interstitial site, and so on.
102 Further investigation on the mechanism of oxygen effect for electrical conduction would
103 be important for the comprehension of intrinsic properties of SnSe.

104 We found that the different electrical conductivity reported by several groups could be
105 intrinsically related to the amount of oxygen content during the synthesis. We succeeded
106 in controlling the transport properties of SnSe single crystals by changing the oxygen
107 amount presented in raw Sn as a surface oxidization. The electrical conducting behavior
108 varied from semiconductor to metal with increase of oxygen amount.

109

110 This work was partly supported by JST CREST Grant No. JPMJCR16Q6, and JSPS
111 KAKENHI Grant No. JP16J05432.

112 ‡Corresponding author: Aichi Yamashita

113 E-mail: YAMASHITA.Aichi@nims.go.jp

114 Postal address: National Institute for Materials Science, 1-2-1 Sengen, Tsukuba, Ibaraki

115 305-0047, Japan

116 Tel.: (+81)29-851-3354 ext. 2976

117

118

119 [1] H. Maier and D. R. Daniel, *J. Electronic Materials* **6**, 693 (1977)

120 [2] Martin Parenteau and Cosmo Carlone, *Phys. Rev. B* **41**, 5227 (1990)

121 [3] Takeshi Inoue, Hidenori Hiramatsu, Hideo Hosono, and Toshio Kamiya, *J. Appl. Phys.*

122 118, 205302 (2015)

123 [4] Li-Dong Zhao, Shih-Han Lo, Yongsheng Zhang, Hui Sun, Gangjian Tan, Ctirad

124 Uher, C. Wolverton, Vinayak P. Dravid & Mercuri G. Kanatzidis, *Nature* **508**, 373

125 (2014)

126 [5] Li-Dong Zhao, Gangjian Tan, Shiqiang Hao, Jiaqing He, Yanling Pei, Hang Chi, Heng

127 Wang, Shengkai Gong, Huibin Xu, Vinayak P. Dravid, Ctirad Uher, G. Jeffrey Snyder,

128 Chris Wolverton, Mercuri G. Kanatzidis, *Science* **351**, 6269 (2015)

129 [6] Yajie Fu, Jingtao Xu, Guo-Qiang Liu, Jingkai Yang, Xiaojian Tan, Zhu Liu, Haiming

130 Qin, Hezhu Shao, Haochuan Jiang, Bo Liang, and Jun Jiang, *J. Mater. Chem. C*, **4**,
131 1201 (2016)

132 [7] J. C. Li, D. Li, X.Y. Qina, J. Zhang, *Scripta Materialia* **126**, 6–10, (2017)

133 [8] Yi Li, Bin He, Joseph P. Heremans, Ji-Cheng Zhao, *Journal of Alloys and*
134 *Compounds* **669**, 224 (2016)

135 [9] Yulong Li, Xun Shi, Dudi Ren, Jikun Chen, and Lidong Chen, *Energies*, **8**, 6275
136 (2015)

137 [10] Xue Wang, Jingtao Xu, Guoqiang Liu, Yajie Fu, Zhu Liu, Xiaojian Tan, Hezhu
138 Shao, Haochuan Jiang, Tianya Tan , and Jun Jiang, *Appl. Phys. Lett.* **108**, 083902
139 (2016)

140 [11] Guodong Tang, Qiang Wen, Teng Yang, Yang Cao, Wei Wei, Zhihe Wang, Zhidong
141 Zhangb and Yusheng Li, *RSC Adv.*, **7**, 8258 (2017)

142 [12] Eyob K. Chere, Qian Zhang, Keshab Dahal, Feng Cao, Jun Mao, and Zhifeng Ren,
143 *J. Mater. Chem. A*, **4**, 1848(2016)

144 [13] Qian Zhang, Eyob Kebede Chere, Jingying Sun, Feng Cao, Keshab Dahal, Shuo
145 Chen, Gang Chen, and Zhifeng Ren, *Adv. Energy Mater.*, **2015**, 1500360 (2015)

146 [14] Hongliang Liu, Xin Zhang, Songhao Li, Ziqun Zhou, Yanqin Liu, and Jiuxing
147 Zhang, *Journal of Electronic Materials*, **46**, (2017)

- 148 [15] M. Gharsallah, F. Serrano-Sánchez, N. M. Nemes, F. J. Mompeán, J. L. Martínez,
149 M. T. Fernández-Díaz, F. Elhalouani & J. A. Alonso, *Scientific Reports* **6**, 26774
150 (2016)
- 151 [16] Anh Tuan Duong, Van Quang Nguyen, Ganbat Duvjir, Van Thiet Duong, Suyong
152 Kwon, Jae Yong Song, Jae Ki Lee, Ji Eun Lee, SuDong Park, Taewon Min,
153 Jaekwang Lee, Jungdae Kim & Sunglae Cho, *Nature Communications* **7**, 13713
154 (2016)
- 155 [17] Kunling Peng, Xu Lu, Heng Zhan, Si Hui, Xiaodan Tang, Guiwen Wang, Jiyan Dai,
156 Ctirad Uher, Guoyu Wang, Xiaoyuan Zhou, *Energy and Environmental Science*, **9**,
157 454-460 (2016)
- 158 [18] Cheng-Lung Chen, Heng Wang, Yang-Yuan Chen, Tristan Day, G. Jeffrey Snyder, J.
159 *Mater. Chem. A*, **2**, 11171-11176, (2014)
- 160 [19] D. Ibrahim, J.-B. Vaney, S. Sassi, C. Candolfi, V. Ohorodniichuk, P. Levinsky, C.
161 Semprimoschnig, A. Dauscher, and B. Lenoir, *Appl. Phys. Lett.* **110**, 032103
162 (2017)
- 163 [20] F. Serrano-Sánchez, M. Gharsallah, N. M. Nemes, F. J. Mompean, J. L. Martínez,
164 and J. A. Alonso, *Appl. Phys. Lett.* **106**, 083902 (2015)
- 165 [21] Niraj Kumar Singh, Sivaiah Bathula, Bhasker Gahtori, Kriti Tyagi, D. Haranath,

- 166 Ajay Dhar, Journal of Alloys and Compounds, **668**, 152-158, (2016)
- 167 [22] S. Sassi, C. Candolfi, J.-B. Vaney, V. Ohorodniichuk, P. Masschelein, A. Dauscher,
168 and B. Lenoir, Appl. Phys. Lett. **104**, 212105 (2014)
- 169 [23] Tian-Ran Wei, Chao-Feng Wu, Xiaozhi Zhang, Qing Tan, Li Sun, Yu Pan and
170 Jing-Feng Li, Phys. Chem. Chem. Phys., **17**, 30102-30109, (2015)
- 171 [24] L. Kövér, Zs. Kovács, R. Sanjinés, G. Moretti, I. Cserny, G. Margaritondo,
172 J. Pálinkás, H. Adachi, Surface and Interface Analysis, **23**, 461-466, (1995)
- 173
- 174

175 Fig. 1 (Color online) Sn 3d_{5/2} XPS spectrum for the surface of grain and powder Sn.

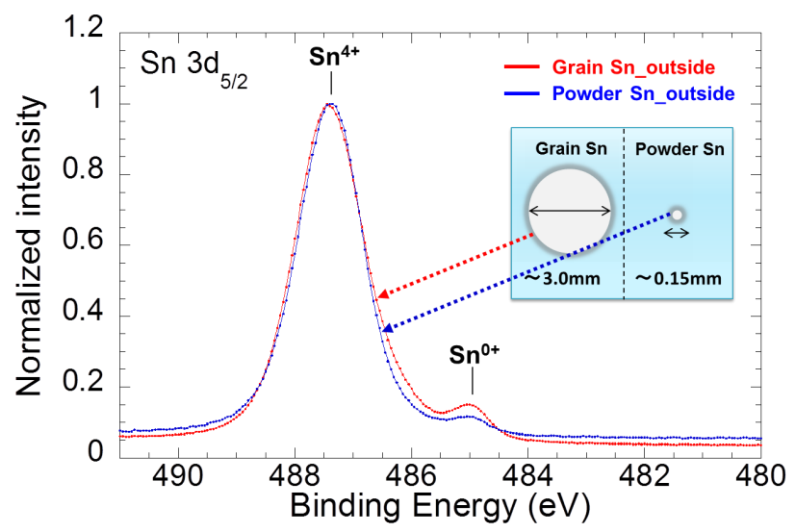
176 Fig. 2 (Color online) XRD patterns of the pulverized SnSe single crystals synthesized

177 from grain and powder Sn.

178 Fig. 3 (Color online) Temperature dependence of the electrical conductivity of SnSe

179 single crystals along the *bc*-plane grown by using different ratio of grain and powder form

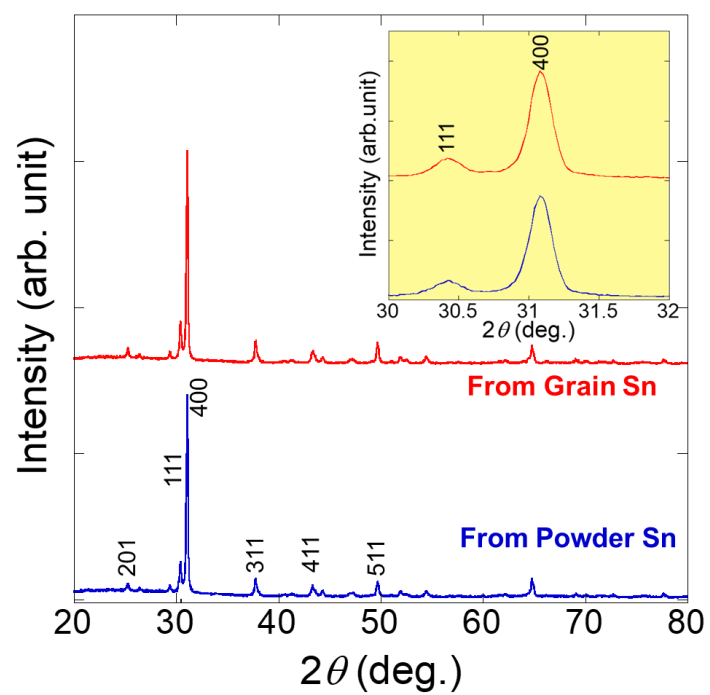
180 Sn as a starting material.



181

182 Fig.1

183

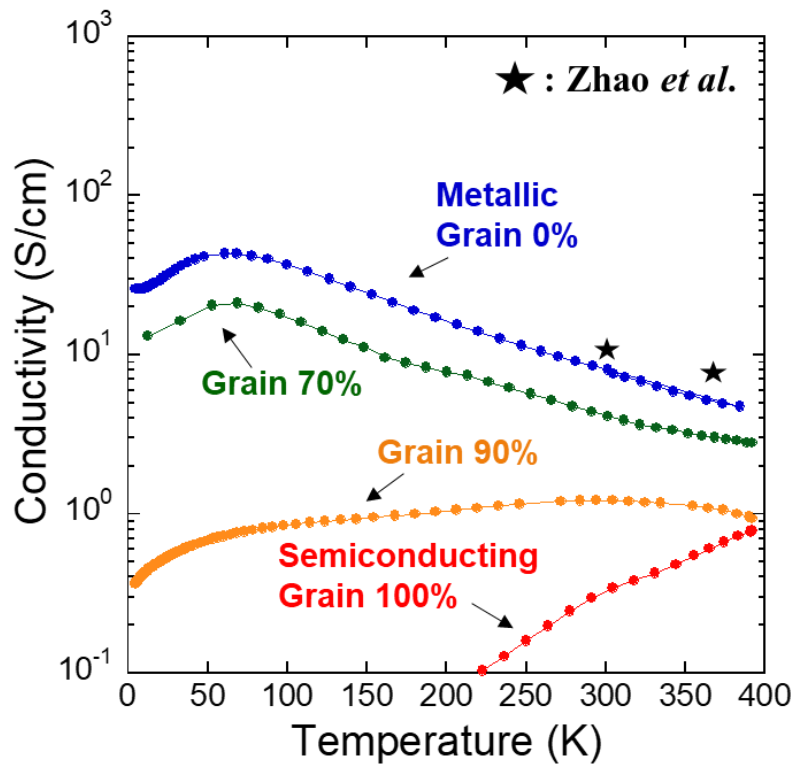


184

185 Fig.2

186

187



188

189

190 Fig.3